

This article was downloaded by:

On: 24 January 2011

Access details: *Access Details: Free Access*

Publisher *Taylor & Francis*

Informa Ltd Registered in England and Wales Registered Number: 1072954 Registered office: Mortimer House, 37-41 Mortimer Street, London W1T 3JH, UK



## Journal of Macromolecular Science, Part A

Publication details, including instructions for authors and subscription information:

<http://www.informaworld.com/smpp/title~content=t713597274>

### Mechanical Behavior of Polyethylene Fibers Reinforced Resol/VAC-EHA

R. K. Misra<sup>a</sup>; Chandan Datta<sup>b</sup>

<sup>a</sup> Department of Mechanical Engineering, B.I.T Mesra, Ranchi, India <sup>b</sup> Department of Polymer Engineering, Birla Institute of Technology, Mesra, Ranchi

**To cite this Article** Misra, R. K. and Datta, Chandan(2009) 'Mechanical Behavior of Polyethylene Fibers Reinforced Resol/VAC-EHA', Journal of Macromolecular Science, Part A, 46: 4, 425 — 437

**To link to this Article:** DOI: 10.1080/10601320902732431

**URL:** <http://dx.doi.org/10.1080/10601320902732431>

PLEASE SCROLL DOWN FOR ARTICLE

Full terms and conditions of use: <http://www.informaworld.com/terms-and-conditions-of-access.pdf>

This article may be used for research, teaching and private study purposes. Any substantial or systematic reproduction, re-distribution, re-selling, loan or sub-licensing, systematic supply or distribution in any form to anyone is expressly forbidden.

The publisher does not give any warranty express or implied or make any representation that the contents will be complete or accurate or up to date. The accuracy of any instructions, formulae and drug doses should be independently verified with primary sources. The publisher shall not be liable for any loss, actions, claims, proceedings, demand or costs or damages whatsoever or howsoever caused arising directly or indirectly in connection with or arising out of the use of this material.

# Mechanical Behavior of Polyethylene Fibers Reinforced Resol/VAC-EHA

R. K. MISRA<sup>1,\*</sup> and CHANDAN DATTA<sup>2</sup>

<sup>1</sup>Department of Mechanical Engineering, B.I.T Mesra, Ranchi, 835215, India

<sup>2</sup>Department of Polymer Engineering, Birla Institute of Technology, Mesra, Ranchi, 835215

Received September 2008; Accepted October 2008

Polyethylene fibers reinforced Resol/VAC-EHA composites have been prepared in the laboratory at different volume fraction of fibers for the evaluation of mechanical properties. Resol solution was blended with vinyl acetate-2-ethylhexyl acrylate (VAc-EHA) resin in an aqueous medium with varying volume fraction of polyethylene fibers. It has also been observed that reinforcement of the polyethylene fiber in Resol/VAC-EHA matrix shows improvement in ductility, tensile strength and Young's modulus. But damping property decreases as soon as percentage of the polyethylene fiber increases. In order to study the static and dynamic response of polyethylene fiber reinforced Resol/VAC-EHA composite plate at uniformly distributed load and fluctuating uniformly distributed load, a multi-quadric radial basis function (MQRBF) method is developed. MQRBF is applied for spatial discretization and a Newmark implicit scheme is used for temporal discretization. The discretization of the differential equations generates a greater number of algebraic equations than the unknown coefficients. To overcome this ill-conditioning, the multiple linear regression analysis, based on the least square error norm, is employed to obtain the coefficients. Simple supported and clamped boundary conditions are considered. Numerical results are compared with those obtained by other analytical methods.

**Keywords:** Polyethylene fiber, resol, multi-quadric radial basis function, vinyl acetate-2-ethylhexyl acrylate (VAc-EHA), damping factor

## Notations

$a, b$	Dimension of plates
$h$	Thickness of plates
$R$	Aspect ratio ( $a/b$ )
$\nu_{LT}$	Major Poisson's ratio
$C_v^*, C_v$	Viscous damping, dimensionless viscous damping
$D_{11}, D_{22}, D_{12}, D_{66}$	Flexural rigidity of plates
$E_L, E_T$	Young's modulus in $x^*, y^*$ direction respectively
$G_{LT}$	Shear modulus relative to $x^* - y^*$ direction
$q, Q$	Transverse load, dimensionless transverse load
$t^*, t$	Time, dimensionless time
$w^*$	Displacement in $z^*$ direction
$w$	Dimensionless displacement in $z$ direction

## 1 Introduction

It is long established fact that fiber reinforced composites have high strength and low weight ratio compared with metals, and hence reduced fuel consumption, longer-range, higher performance or greater payload in aircraft. Blending of fibers with matrix is an effective approach to obtain material with specific mechanical properties (1). But good polymer/fiber interaction (2) is important to enhance the strength and modulus.

Polyethylene fibers reinforced composites are gaining importance due to various advantages of polyethylene fibers these are excellent ductility, resistance to wear and moisture, low density and better tensile strength. But Polyethylene fibers have some drawbacks also, these are lower compressive properties, poor adhesion to resin matrices and low creep resistance (3–8), which limit its applications.

The interfacial shear strength of the polyethylene fibers reinforced composites falls between the glass fibers reinforced polyester and epoxy resin. Due to high shear strength, polyethylene fibers reinforced composites are reasons for further investigations.

As compared to polyethylene fibers reinforced thermosetting composites, polyethylene fibers reinforced thermoplastic polymer matrices and thermoplastic-thermoset

\*Address correspondence to: R. K. Misra, Department of Mechanical Engineering, B.I.T Mesra, Ranchi, 835215, India. Tel.No. +919431382611; E-mail: mishrark.kanpur@yahoo.com

interpenetrating network (IPN) polymer matrices composites potentially offer several advantages. The properties of the resol improve by blending vinyl acetate-2-ethylhexyl acrylate copolymer (VAc-EHA) by IPN technique. It has vast applications in military and commercial aircraft.

Thermoset Phenolic resin possesses excellent fire retardancy and low smoke density (9–11) property. But its application is limited due to its brittleness. Various efforts have been done to increase its toughness.

The polyester-phenolic copolymer has been synthesized to improve the mechanical properties and heat resistance (12). The flexural strength of the thermoset phenolic resin improves when it is blended with resol-type phenolic resin (13).

Composites are replacing metals in structural applications. Therefore, it is important to predict the static and dynamic behavior of the composite when it is used in structural applications. The theoretical analysis of polyethylene fiber reinforced composite plates by conventional methods poses some problems. Normally finite element method is very popular to analyze the behavior of composites, but it is not suitable as it consumes more time in mesh generation than in execution. Due to this problem, researchers developed new methods. These are known as meshless methods.

In this paper, after fabrication and evaluation of the mechanical properties of unidirectional polyethylene fibers reinforced Resol/VAc-EHA composites at different volume fraction of the fibers, meshless multiquadric radial basis function (MQRBF) method is employed for static and dynamic analysis of polyethylene fibers reinforced Resol/VAc-EHA Composite plate. In 1971, Hardy (14) used the MQRBF for the scattered data interpolation. After that Kansa (15) developed the concept of solving partial differential equations using radial basis function (RBF). Franke (16) studied the evaluation of RBF's for scattered data interpolation in terms timing, accuracy and ease of implementation. Coleman (17) applied the radial basis function for the analysis of elliptic boundary value problems. Ferreira applied the radial basis function for the analysis of composite beams (18) and plates (19). Misra et al. (20–21) used this method for the analysis of anisotropic plates and laminate. Frank and Schaback (22) developed the concept of solving PDEs using radial basis functions (RBF). Fedoseyev et al. (23) improved the accuracy of the solution by placing the interior knots.

The dynamic behavior of unidirectional banana fibers reinforced high-density polyethylene/ poly( $\epsilon$ -caprolactone) composites using MQRBF have been presented by Misra et al. (24).

## 2 Experimental

### 2.1 Materials

Resol was prepared by the method cited in the literature (25–26). The hardener for resol was para-toluene sulphonic

acid (PTSA), 0982 H from Bakelite AG. VAc-EHA copolymer in emulsion form was obtained from Macromoles, India. Hydroxy methoxy methyl melamine (HMMM) was prepared in the laboratory using a standard procedure (27). PEF (Spectra 900, 1200 den) supplied by Allied-Signal Corporation, Petersburg, USA.

### 2.2 Treatment of Polyethylene Fiber

For the use of treated fiber in making composites, the fibers were immersed in chromic acid at room temperature for 15 min (28), after which they were immediately rinsed in distilled water followed by washing in running water for 2 h. The fibers were then given a further immersion in distilled water and dried in an air oven at 40°C for 5 h. For these treatments, the standard composition of chromic acid adopted (29–33) was Potassium dichromate (7 parts), concentrated sulphuric acid (150 parts) and water (7 parts).

### 2.3 Preparation of Composites

The individual polymers (Resol and vinylacetate-2-ethylhexyl acrylate copolymer) were first separately diluted with distilled water to maintain a solid content of 50% by weight for convenience, under well-stirred condition. Then a weighed amount of resol was taken in a three-necked round bottom flask. VAc-EHA copolymer was then accurately weighed into the flask and the contents were stirred to give a homogeneous mixture in the desired blend ratio of the components. Para-toluene sulfonic acid (PTSA) 7% by weight based on resol [34] was thoroughly mixed for 20 min. Then hydroxy methoxy methyl melamine (HMMM) was added at 20% by weight of VAc-EHA copolymer.

The prepegs of polyethylene fiber (PEF) were prepared previously. When the formation of the bubbles ceased, the viscous mass was poured into a glass mold prepared by clipping together two glass plates separated by a Teflon gasket in between, the thickness of which controls the thickness of the sample sheet formed. It was then initially kept at room temperature for about 24 h and then heated at 80°C for 4 h (35). Thus, the samples were produced.

### 2.4 Tensile Properties

An Instron universal – testing machine (Model 3360) was used for measuring the tensile properties like tensile strength, modulus. ASTM D638 method was followed. A crosshead speed of 5 mm/min was maintained. All testing were conducted under ambient conditions in an environmentally controlled room. The data reported are averages of at least six measurements, and typical scattering range of the results was  $\pm 5\%$ .

### 2.5 Theoretical Analysis

After evaluating the mechanical properties of the unidirectional polyethylene fibers reinforced Resol/VAC-EHA composites at different volume fraction of the fibers, Multiquadric radial basis function method is applied for static and dynamic analyses of the unidirectional polyethylene fibers reinforced Resol/VAC-EHA composite plate to assess its response to external loading such as uniformly distributed load.

### 2.6 Multiquadric Radial Basis Function Method

Consider a general differential equation:

$$Aw = f(x, y) \quad \text{in } \Omega \quad (1)$$

$$Bw = g(x, y) \quad \text{on } \partial\Omega \quad (2)$$

where  $A$  is a linear differential operator and  $B$  is a linear boundary operator imposed on boundary conditions for the orthotropic plate.

In the present research work, it is assumed that the polyethylene fiber reinforced composite plate behaves as an orthotropic plate since the diameter of polyethylene fiber is so small that its contribution to the strength is predominantly along its longitudinal direction only.

Let  $\{P_i = (x_i, y_i)\}_{i=1}^N$  be  $N$  collocation points in domain  $\Omega$  of which  $\{(x_i, y_i)\}_{i=1}^{N_f}$  are interior points;  $\{(x_i, y_i)\}_{i=N_f+1}^N$  are boundary points. In MQRBF method, the approximate solution for differential equation (1) and boundary conditions (2) can be expressed as:

$$w(x, y) = \sum_{j=1}^N w_j \varphi_j(x, y) \quad (3)$$

and multi-quadric radial basis as:

$$\varphi_j = \sqrt{(x - x_j)^2 + (y - y_j)^2 + c^2} = \sqrt{r_j^2 + c^2} \quad (4)$$

where  $\{w_j\}_{j=1}^N$  are the unknown coefficients to be determined, and  $\varphi_j(x_j, y_j)$  is a basis function. Other widely used radial basis functions are:

$\varphi(r) = (c^2 + r^2)^{1/2}$	Multiquadrics
$\varphi(r) = (c^2 + r^2)^{-1/2}$	Inverse multiquadrics
$\varphi(r) = r^3$	Cubic
$\varphi(r) = r^2 \log(r)$	Thin plate splines
$\varphi(r) = (1 - r)_+^m p(r)$	Wendland functions
$\varphi(r) = e^{-(cr)^2}$	Gaussian

Here  $c$  is a shape parameter, a positive constant. Ling and Kansa (36) discussed about the shape parameter.

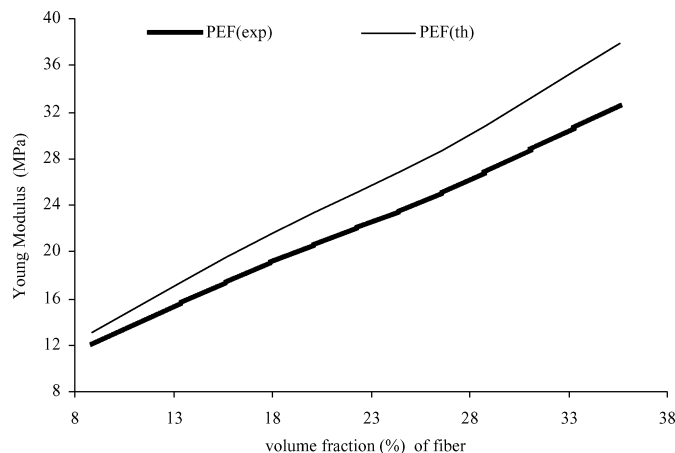


Fig. 1. Theoretical and experimental modulus of elasticity of the polyethylene fiber reinforced composites in longitudinal direction at different volume fraction of the fiber.

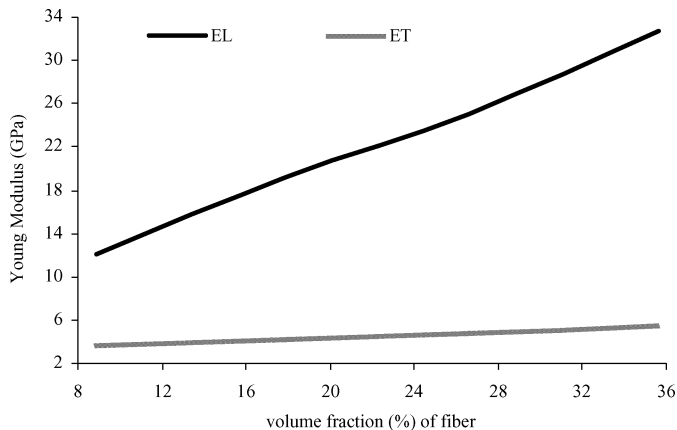
### 3 Results and Discussion

Theoretical and experimental Young’s modulus of the polyethylene fiber reinforced composites in longitudinal direction at different volume fraction of the fibers has been shown in Figure 1. Young’s modulus ( $E_L$ ) appears to be linearly dependent on volume fraction of the fibers ( $V_f$ ). As soon as volume fraction of the fiber increases theoretical and experimental Young’s modulus increases, but theoretical Young’s modulus increases at higher rate as compared to experimental Young’s modulus.

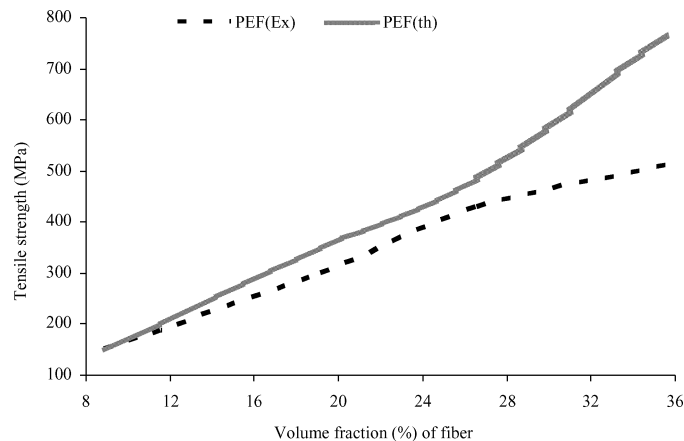
The interesting feature of this study is that the distance between corresponding theoretical and experimental curves increases with  $V_f$ , and the deviation is minimum at lower range of  $V_f$ . In the present work, the hand lay-up technique has been used with a  $V_f$  range of 0.089–0.356. At a higher  $V_f$ , fiber interaction takes place, and either they tend to bundle up among themselves or they touch each other physically, which is due to the fact that hand lay-up technique produces more or less random nature of fiber distribution in the matrix. Due to the above facts, proper and uniform penetration of the matrix does not take place throughout the fiber surfaces, leaving interstitial voids. Thus, the degree of fiber misalignment and void content increases with the increase in  $V_f$ . These facts are reflected in the experiment by the deviation of the experimental curve from the theoretical one.

Figure 2 shows the longitudinal and transverse modulus of elasticity of the polyethylene fiber reinforced composites at different volume fraction of the fibers. When volume fraction of the fibers is 8.9% difference between both Young’s modulus is less but as soon as volume fraction of the fiber increases difference between both Young’s modulus also increases.

Stress- strain behavior of the polyethylene fiber reinforced composites and Resol/VAC-EHA matrix has been



**Fig. 2.** Longitudinal and transverse modulus of elasticity of the polyethylene fiber reinforced composites at different volume fraction of the fibers.



**Fig. 4.** Experimental and theoretical tensile strength of the polyethylene fiber reinforced composites at different volume fraction of the fibers.

shown in Figure 3. As soon as percentage of the polyethylene fiber increases in composite plate tensile stress of the composite plate also increases. The stress-strain curve display a point of inflection (Knee point) around  $\epsilon_m$ , which enables the curve to be approximated by two regions – one indicating the elastic (below the point corresponding to  $\epsilon_m$ ), other the plastic region (beyond the point corresponding to  $\epsilon_m$ ). It is established that the elastic region of the composite is dependent on  $\epsilon_m$ . The increase in fiber content leads to an increase in the first crack stress (corresponding to  $\epsilon_m$ ), and the ultimate strain. It is observed from the stress-strain curves that the main influence of the fibers is in the post-cracking zone, where the contribution of the matrix is small or even negligible.

The experimental and theoretical tensile strength of the polyethylene fiber reinforced composites has been shown in Figure 4 at different volume fraction of the fibers. From

the graph it is established that the elastic region of the composite is dependent on matrix.

The increase in fiber content leads to an increase plastic deformation. The experimental tensile strength is less than theoretical tensile strength. It is observed that upto 26.6% volume fraction of the fiber difference between experimental and theoretical tensile strength is less but as soon as % volume fraction of the fiber increases above 26.6%, the theoretical tensile strength increase at higher rate as compared to experimental tensile strength.

Figure 5 shows the elongation at break of the polyethylene fiber reinforced composites at different volume fraction of the fibers. It is observed that elongation shows linear relationship upto 17.9% volume fraction of the fibers but becomes constant from 17.9% to 26.6% volume fraction of fibers and after 26.6% volume fraction of fibers it increases slowly.

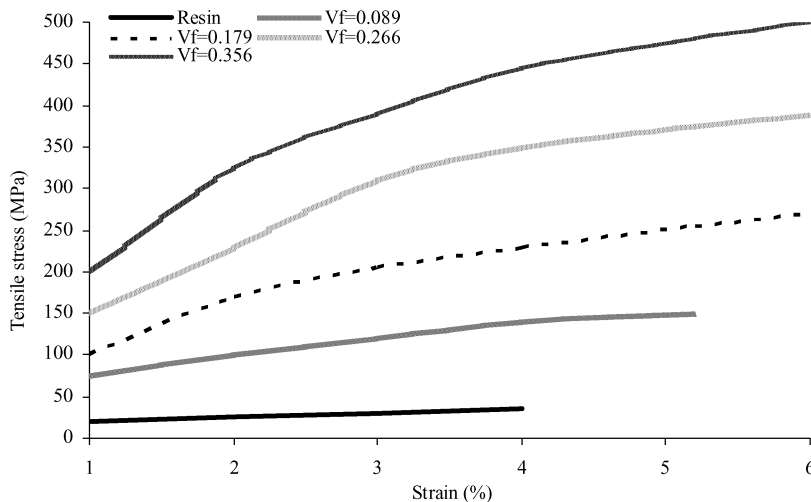


**Fig. 3.** Stress-strain behavior of the polyethylene fiber reinforced composites and Resol/VAC-EHA matrix.

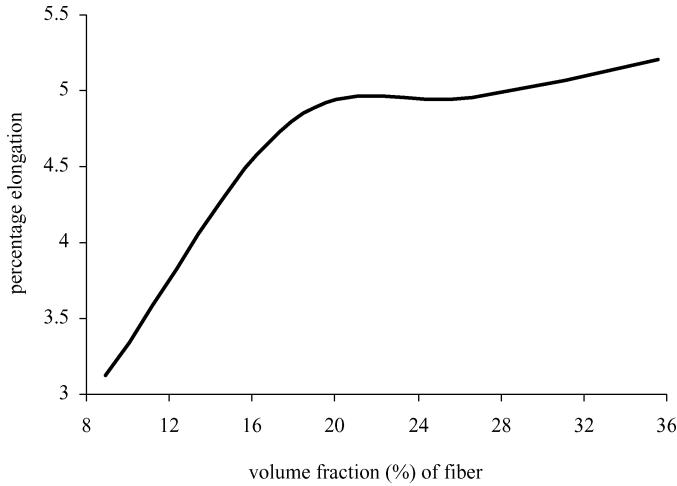


Fig. 5. Elongation of the polyethylene fiber reinforced composite at different volume fraction of the fibers.

Table 1 shows the tensile modulus of the polyethylene fibers reinforced in Resol/VAC-EHA composites at different volume fraction of the fibers. As volume fraction of fiber increases from 8.9% up to 35.6%, longitudinal modulus of elasticity increases 58.67%, 107.4380% and 170.24%, respectively.

Table 2 presents the comparison of mechanical properties between polyethylene (PE) fibers reinforced Resol/VAC-EHA composites and other reported polyethylene fibers reinforced composites. After comparing the various polyethylene fiber reinforced composites, it is observed that PE fibers reinforced Resol/VAC-EHA composites have better mechanical properties as compared to PE fiber reinforced LDPE composites (37). But mechanical properties of the PE fiber reinforced PE composites are better than PE fibers reinforced Resol/VAC-EHA composites (38).

3.1 Case Study: Static and Dynamic Response of the Composite plate

Figure 6 shows the geometry, coordinate system and loading polyethylene in fiber reinforced composites. Neglecting the transverse shear and rotary inertia, equation of polyethylene fiber reinforced composites is expressed in

Table 1. Mechanical properties of the polyethylene fibers reinforced in Resol/VAC-EHA (F20) Composites

Code	Volume fraction of fiber in percentage (%)	$E_L$ (GPa)	$E_T$ (GPa)	Percentage (%) Elongation at break
F20PE8.9	8.9	12.1	3.66	3.25
F20PE17.9	17.9	19.2	4.27	5.69
F20PE26.6	26.6	25.1	4.9	6.78
F20PE35.6	35.6	32.7	5.6	6.84

Table 2. Mechanical properties of the various polyethylene fiber based composites

Measured properties of Composite Materials	Polyethylene fiber reinforced Resol/VAC-EHA Composites fiber content Polyethylene 35.6% by volume	Reported Polyethylene based fiber composites
Tensile strength (MPa)	510	28.72 [37] 1300 [38]
Longitudinal Tensile Modulus (GPa)	32.7	0.737 [37]
% Elongation at break	6.84 %	4.25 % [37] 3.5% [38]

non-dimensional form as:

$$(w_{xxxx} + 2R^2\eta w_{xxyy} + R^4\psi w_{yyyy}) + w_{tt} + c_v w_t - Q(x, y, t) = 0 \tag{5}$$

where the subscript denotes the partial derivative with respect to the suffix following. The non-dimensional quantities are defined by:

$$w = w^*/h, x = x^*/a, y = y^*/b, R = a/b,$$

$$t = t^* \sqrt{D_{11}/(\rho a^4 h)}$$

$$Q = qa^4/(D_{11}h), C_v = (C_v^*/M)\sqrt{(\rho a^4 h)/D_{11}}, M = \rho abh$$

$$\eta = (D_{12} + 2D_{66})/D_{11}, \psi = D_{22}/D_{11} \tag{6}$$

Boundary conditions for the plate simply supported at all four edges are:

$$x = 0, 1 \quad w = 0 \tag{7a}$$

$$x = 0, 1 \quad w_{xx} = 0 \tag{7b}$$

$$y = 0, 1 \quad w = 0 \tag{7c}$$

$$y = 0, 1 \quad w_{xx} = 0 \tag{7d}$$

Boundary conditions for the clamped edge plate are:

$$x = 0, 1 \quad w = 0 \tag{8a}$$

$$x = 0, 1 \quad w_x = 0 \tag{8b}$$

$$y = 0, 1 \quad w = 0 \tag{8c}$$

$$y = 0, 1 \quad w_y = 0 \tag{8d}$$

The governing Equation 5 is solved using multi-quadratic radial basis function and boundary conditions, Equations 7 and 8, for simply supported and

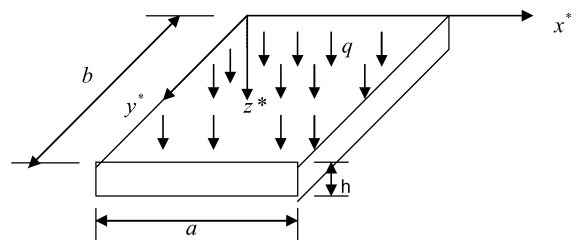


Fig. 6. Geometry of the polyethylene fiber reinforced Resol/VAC-EHA blend composite plate.

Downloaded At: 09:34 24 January 2011

**Table 3.** Deflection of the simple supported polyethylene fibers reinforced Resol/VAC-EHA Composite plate at 8.9% volume fraction of the fibers

$q$ ( $N/m^2$ )	$b$ (mm)	$a$ (mm)	$b/a$	$h$ (mm)	Whitney [31], $m=1, n=1$	MQRBF Method
					$w_{max}$ (mm)	$w_{max}$ (mm)
10	300	300	1.0	10	4.3517e-004	4.288e-04
10	300	150	2.0	10	5.6743e-005	5.828e-05
10	300	100	3.0	10	1.3593e-005	1.330e-05

**Table 4.** Deflection of the simple supported polyethylene fibers reinforced Resol/VAC-EHA Composite plate at 17.9% volume fraction of the fibers

$q$ ( $N/m^2$ )	$b$ (mm)	$a$ (mm)	$b/a$	$h$ (mm)	Whitney [31], $m=1, n=1$	MQRBF Method
					$w_{max}$ (mm)	$w_{max}$ (mm)
10	300	300	1.0	10	2.8626e-004	2.871e-004
10	300	150	2.0	10	3.6268e-005	3.693e-005
10	300	100	3.0	10	8.6428e-006	8.440 e-006

**Table 5.** Deflection of the simple supported polyethylene fibers reinforced Resol/VAC-EHA Composite plate at 26.6% volume fraction of the fibers

$q$ ( $N/m^2$ )	$b$ (mm)	$a$ (mm)	$b/a$	$h$ (mm)	Whitney [31], $m=1, n=1$	MQRBF Method
					$w_{max}$ (mm)	$w_{max}$ (mm)
10	300	300	1.0	10	2.2225e-004	2.249e-004
10	300	150	2.0	10	2.7876e-005	2.866e-005
10	300	100	3.0	10	6.6312e-006	6.469 e-006

**Table 6.** Deflection of the simple supported polyethylene fibers reinforced

$q$ ( $N/m^2$ )	$b$ (mm)	$a$ (mm)	$b/a$	$h$ (mm)	Whitney [31], $m=1, n=1$	MQRBF Method
					$w_{max}$ (mm)	$w_{max}$ (mm)
10	300	300	1.0	10	1.7287e-004	1.758e-004
10	300	150	2.0	10	2.1488e-005	2.154e-005
10	300	100	3.0	10	5.1036e-006	4.922e-006

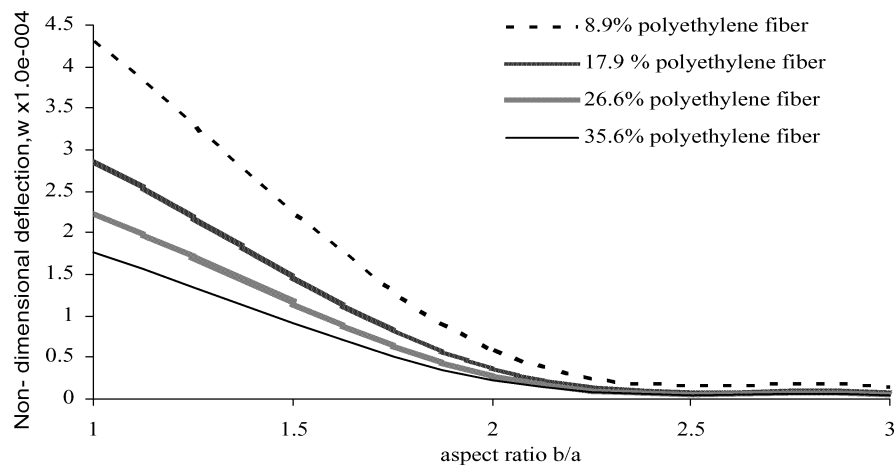


**Fig. 7.** Deflection of the simple supported polyethylene fiber reinforced

Downloaded At: 09:34 24 January 2011

**Table 7.** Deflection of the clamped edge polyethylene fibers reinforced Resol/VAC-EHA Composite plate at different volume fraction of the fibers

	% Volume fraction of fiber	Whitney [31], $m = 1, n = 1$	
		$w_{max}(mm)$	MQRBF Method $w_{max}(mm)$
$q = 10 (N/m^2)$	8.9 %	1.5026e-004	1.549 e-004
$a = b = 300 (mm)$	17.9%	1.0016e-004	1.028 e-004
$h = 10 mm$	26.6%	7.8138e-005	7.996 e-005
	35.6%	6.1040e-005	6.238e-005

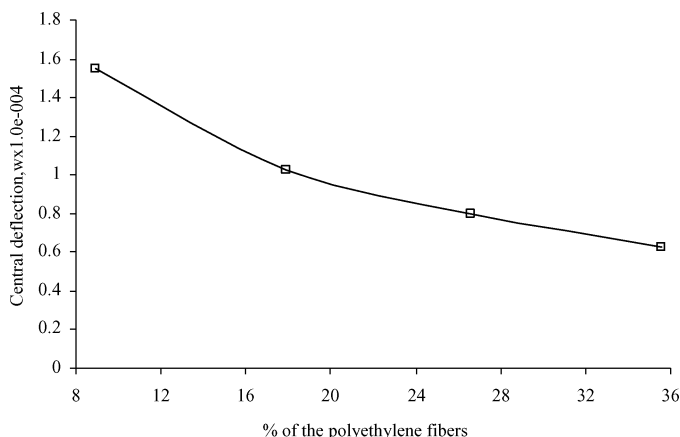


**Fig. 8.** Deflection of the clamped edge polyethylene fiber reinforced composite plate at different % of the polyethylene fibers.

clamped edge plates respectively, and has been presented in Appendix A. In this multi-quadric radial basis function method number of algebraic equations creates more than the number of unknown coefficients  $\{w_j\}_{j=1}^N$ . Hence, this method creates ill conditioning. To over-

come this ill-conditioning, multiple linear regressions analysis (Appendix B) based on least-square error norms is employed.

Deflection of the polyethylene fiber reinforced composite plate at various aspect ratios of the present method for simply supported boundary condition has been compared with those obtained by Whitney (39) as shown in Tables 3–6. Figure 7 shows the behavior of polyethylene fiber reinforced composite plates at different volume fraction of the polyethylene fibers. There is good agreement between the present results and reference solution. The following features are observed after analyzing the Tables 3–6 and Figure 7 for simple supported boundary conditions:

As aspect ratio increases deflection decreases due to decrease in load.

After aspect ratio 2, difference in deflection is very less of polyethylene fiber reinforced composite plates at different volume fraction of the polyethylene fibers.

8.9% polyethylene fiber reinforced composite plate gives maximum deflection and 35.6% polyethylene fiber reinforced composite plate gives least deflection. It means strength of the 8.9% polyethylene fiber reinforced composite plate is least and 35.3% glass fiber reinforced composite plate is maximum.

Similar behavior is observed at clamped edge boundary conditions as shown in Table 7 and Figure 8, but clamped edge plate deflect less as compared to simple supported plate. As soon as percentage of the polyethylene fiber increases in clamped edge polyethylene fiber reinforced composite plate, deflection decreases at slower rate as compared to simple supported polyethylene fiber reinforced composite plate.

A computer program based on the finite difference method (FDM) proposed by Chadrashekara (40) is also developed. The dynamic response of the simple supported composite plates obtained by the present method and finite difference method has been compared and shown in Figure 9 at uniformly distributed load  $q = 10 (N/m^2)$ , sides  $a = b = 300 (mm)$  and thickness  $h = 10 (mm)$ . There is good agreement in the results. The following features are observed after analyzing the Figure 10–15 for the simple supported boundary condition:

8.9% polyethylene fiber reinforced Resol/VAC-EHA blend square composite plate takes less time to stabilize

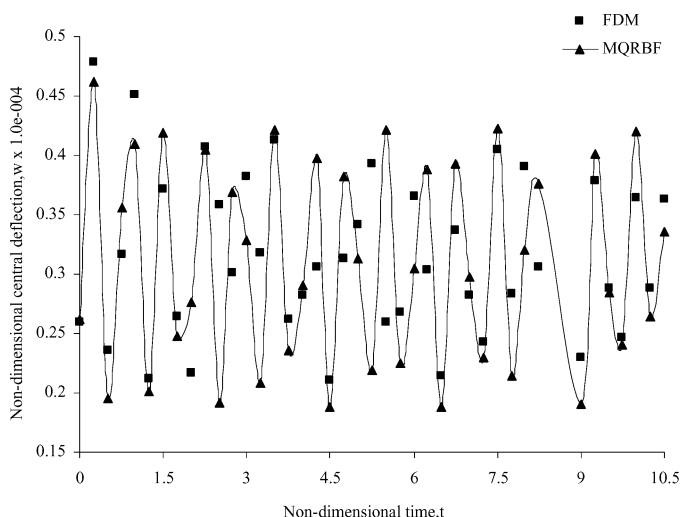


**Fig. 9.** Dynamic response of the simple supported polyethylene fiber reinforced Resol/VAC-EHA blend composite plate at uniformly distributed load  $q = 10 N/m^2$ .



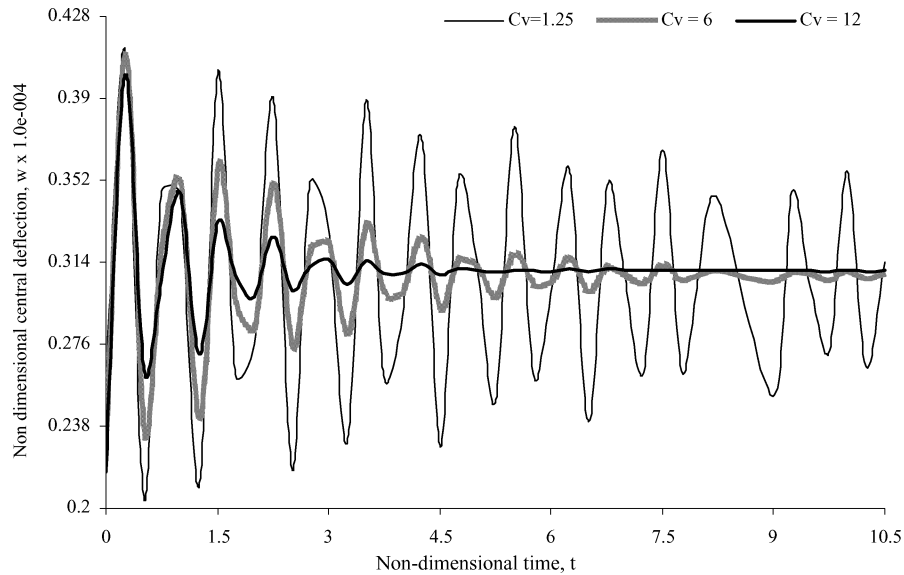


**Fig. 10.** Damped response of a simple supported 8.9% polyethylene fiber reinforced Resol/VAC-EHA blend square composite plate at various damping coefficient factor and uniformly distributed load  $q = 10 \text{ N/m}^2$ .

as compared to 35.6% polyethylene fiber reinforced Resol/VAC-EHA blend square composite plate.

As soon as percentage of the polyethylene fiber increases from 8.9% up to 35.6% damping property of the composite plate decreases.

At the same volume fraction, aspect ratio ( $b/a$ ) of the polyethylene fiber reinforced composite plate increases stability time also increases.

At the same volume fraction, maximum non-dimensional deflection due to fluctuating uniformly dis-

tributed load ( $5 \text{ N/m}^2$  to  $10 \text{ N/m}^2$ ) in polyethylene fiber reinforced composite plate is less as compared to uniformly distributed load  $q = 10 \text{ N/m}^2$  as shown in Figures 12 and 10.

At damping coefficients factor  $C_v = 1.25$ , maximum non-dimensional deflection are 0.4126, 0.2619, 0.1993, 0.1522 in 8.9%, 17.9%, 26.6% and 35.6% polyethylene fiber reinforced composite plate, respectively.

When the damping coefficient factor increases from 1.25–12, non-dimensional deflection decreases.

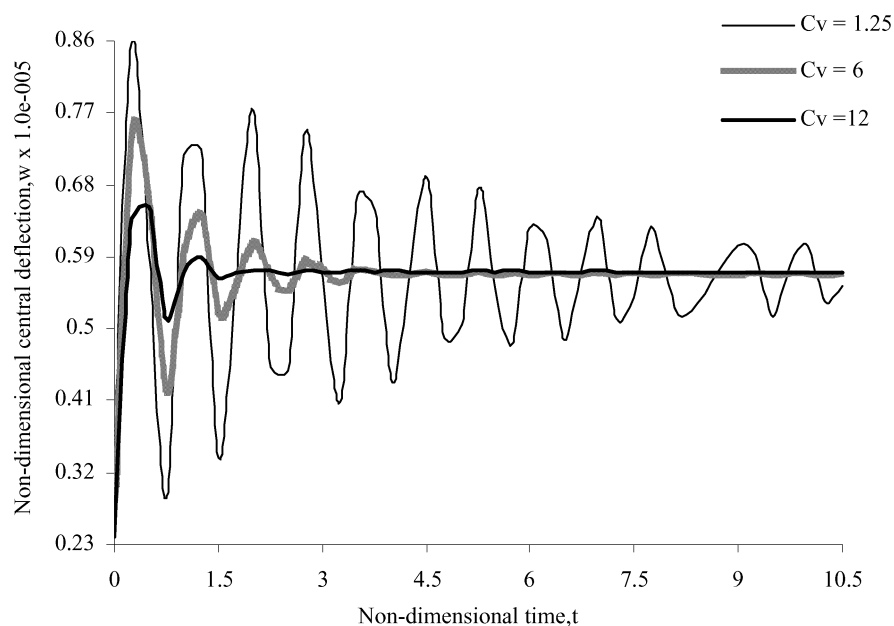


**Fig. 11.** Damped response of a simple supported 8.9% polyethylene fiber reinforced Resol/VAC-EHA blend composite plate at aspect ratio  $b/a = 2.0$  and uniformly distributed load  $q = 10 \text{ N/m}^2$ .

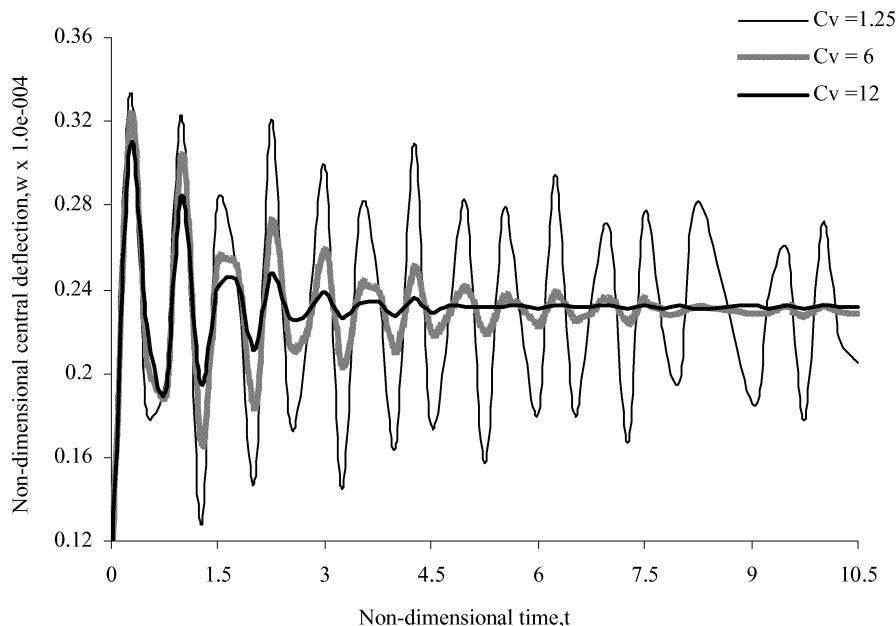


**Fig. 12.** Damped response of a simple supported 8.9% polyethylene fiber reinforced Resol/VAC-EHA blend square composite plate at fluctuating uniformly distributed load from 5 N/m<sup>2</sup> to 10 N/m<sup>2</sup>.

It may be noted here that after introducing the polyethylene fibers, the tensile strength of the composite increases, therefore the maximum non-deflection decreases in polyethylene fiber reinforced composite plate. Pothan et al. (41) reported that in a composite system, damping is affected through the incorporation of fibers. This is due mainly to shear stress concentrations at the fiber ends in association with the additional visco-elastic energy dissipation in the matrix material. Another contributing factor

could be the elastic nature of the fiber. When interfacial bonding improves, damping property decreases.

Similar behavior is observed at clamped edge boundary conditions as shown in Figure 18, but clamped edge plate takes more time to stabilize as compared to simple supported plate because clamped edge plate dissipate less energy and second important point is, maximum non-dimensional deflection is less in clamped edge plate as compared to simple supported plate.

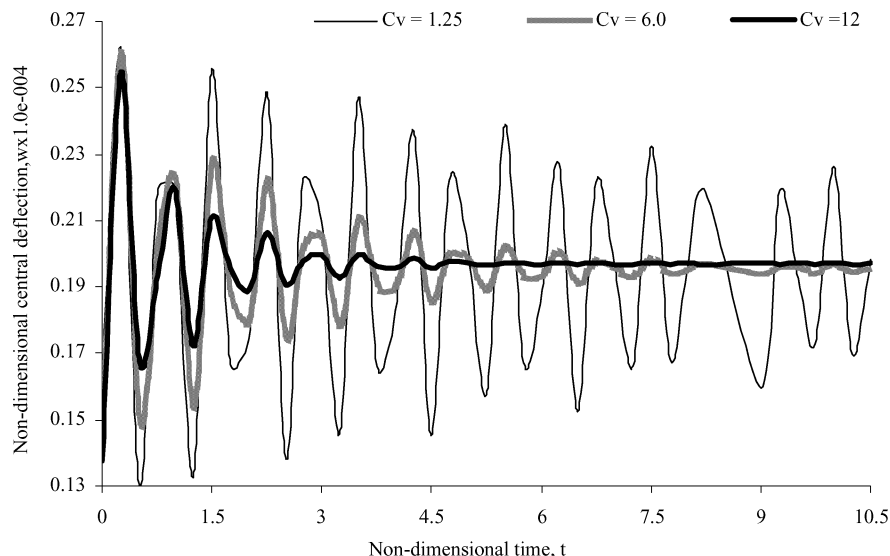


**Fig. 13.** Damped response of a simple supported 17.9% polyethylene fiber reinforced Resol/VAC-EHA blend square composite plate at various damping coefficient factor and uniformly distributed load  $q = 10 \text{ N/m}^2$ .

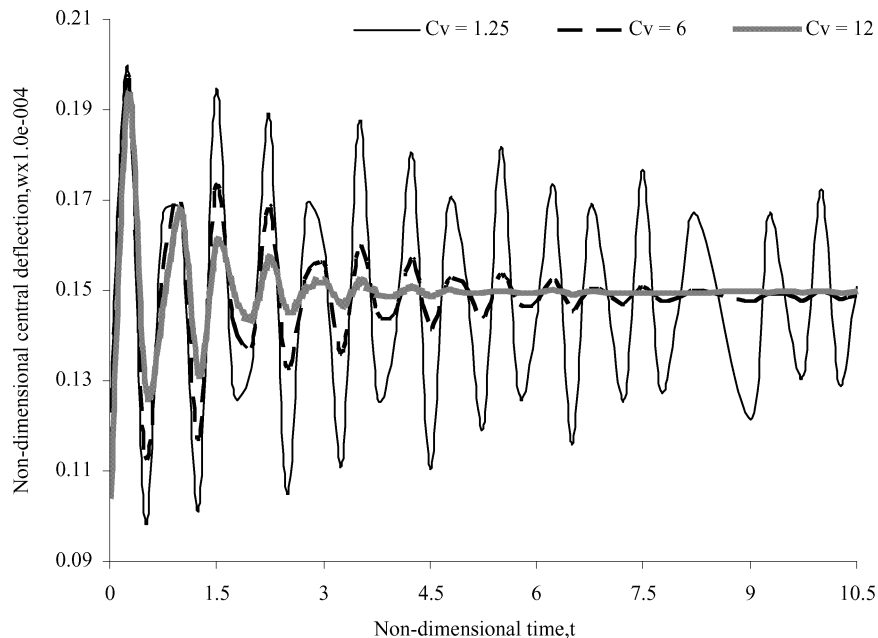


**Fig. 14.** Damped response of a simple supported 26.6 % polyethylene fiber reinforced Resol/VAC-EHA blend square composite plate at various damping coefficient factor and uniformly distributed load  $q = 10 \text{ N/m}^2$ .

Figures 16 and 17 show the transverse velocity and transverse acceleration of simple supported polyethylene fiber reinforced Resol/VAC-EHA blend square composite plate at different volume fraction of the fibers. It is observed that 8.9% polyethylene fiber reinforced composite plate gives maximum transverse velocity and acceleration and 35.6% polyethylene fiber reinforced composite plate gives least

transverse velocity and acceleration. Two factors plays important role for variation in velocity and acceleration. One is uniformly distributed load which always decrease the velocity and acceleration and other is visco-elastic internal forces of the composite plate which act opposite to uniformly distributed load. It tries to increase the velocity and

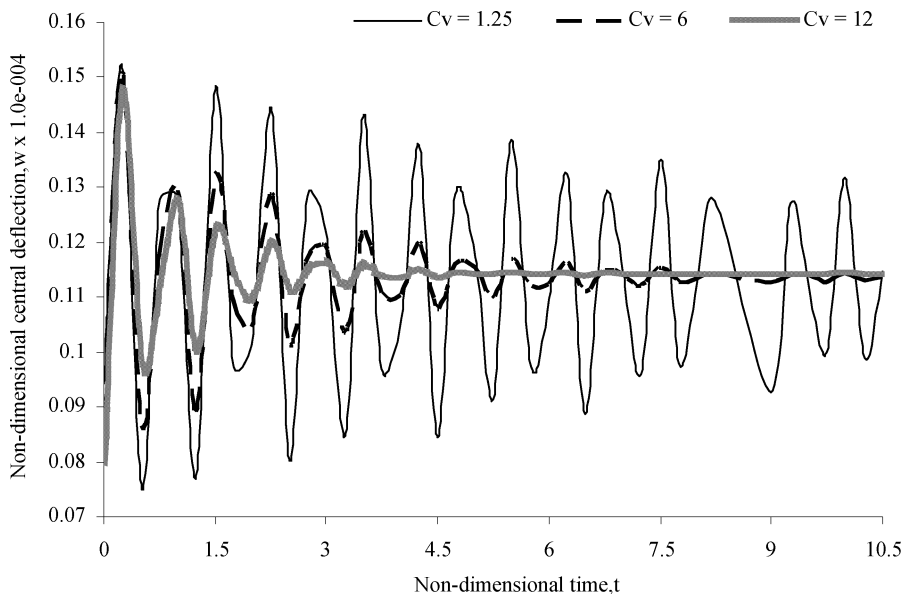


**Fig. 15.** Damped response of a simple supported 35.6% polyethylene fiber reinforced Resol/VAC-EHA blend square composite plate at various damping coefficient factor and uniformly distributed load  $q = 10 \text{ N/m}^2$ .

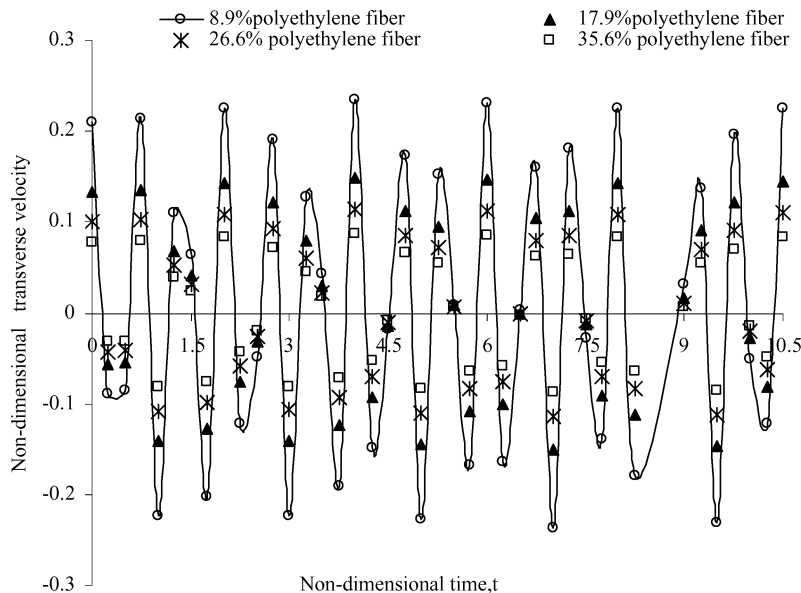


**Fig. 16.** Transverse velocity of a simple supported polyethylene fiber reinforced Resol/VAC-EHA blend square composite plate at uniformly distributed load  $q = 10 \text{ N/m}^2$ .

acceleration. Due to this reason, there is variation in velocity and acceleration.

**4 Conclusions**

Polyethylene fiber reinforced Resol/VAC-EHA composites plate has been prepared in laboratory to evaluate their mechanical properties. Theoretical static and dynamic analyses of the composite plate have also been presented in this work. Reinforcement of polyethylene fibers into the Resol/VAC-EHA matrix shows improvement in ductility, tensile strength and Young’s modulus. But as soon as per-

centage of the polyethylene fibers increase, damping properties decrease. At low percentage of the polyethylene fiber in composite, elongation shows linear relationship. It becomes constant at higher percentage of the polyethylene fiber in composite.

Furthermore, the multi quadric radial basis function method is used to analyze the static and dynamic behavior of the polyethylene fiber reinforced Resol/VAC-EHA composites plate. In this collocation method, the number of equations generated is more than the number of unknowns. Therefore, multiple regression analysis is used to overcome this incompatibility. This method is found to be effective in static and dynamic response of the composite plates.

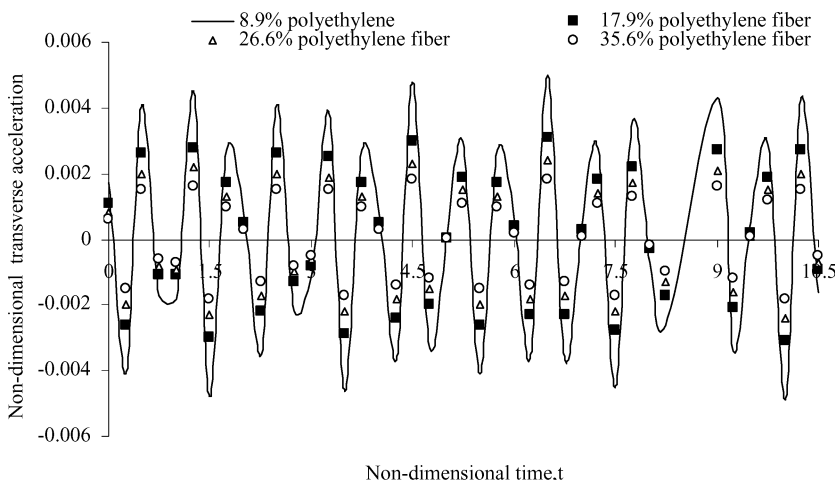


**Fig. 17.** Transverse acceleration of a simple supported polyethylene fiber reinforced Resol/VAC-EHA blend square composite plate at uniformly distributed load  $q = 10 \text{ N/m}^2$ .

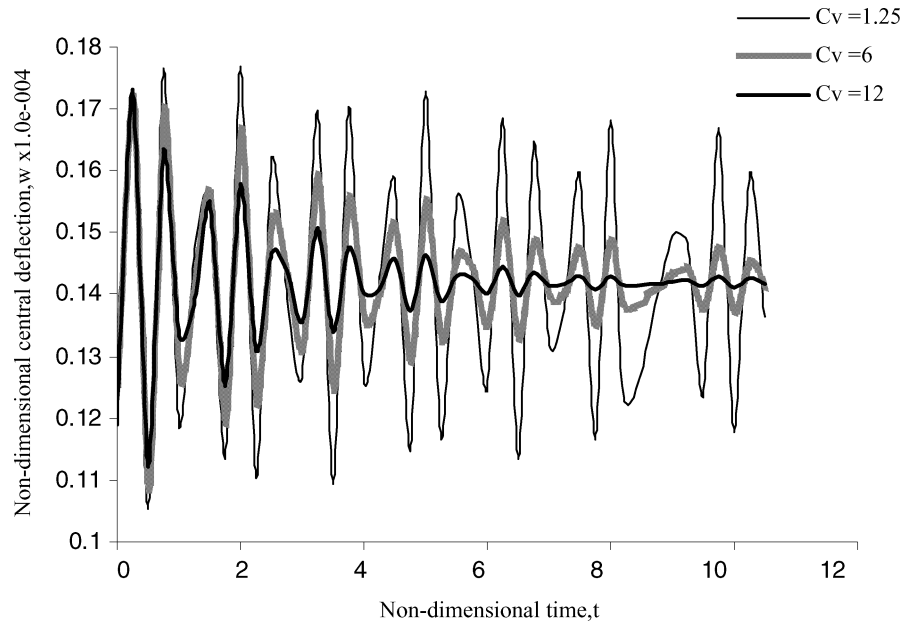


**Fig. 18.** Damped response of a clamped edge 8.9% polyethylene fiber reinforced Resol/VAC-EHA blend square composite plate at various damping coefficient factor and uniformly distributed load  $q = 10 \text{ N/m}^2$ .

## References

1. Yang, M.B., Li, Z.M. and Feng, J.M. (1998) *Polym. Eng. Sci.*, 38, 879–883.
2. Chawla, K.K. Composite Materials: Science and Engineering, First edition. Springer: New York, 1987.
3. Nguyen, HX. (1990) *Sea. Tech.*, 31, 31–35.
4. Wincklhofer, R.C. and Rothwell, R.E. (1986) *Oceans*, 18, 278–283.
5. Gibson, R.F., Vidish, S. and Mantena, R. Vibration damping characteristics of highly oriented polyethylene fiber reinforced epoxy composites, International SAMPE Symposium and Exhibition, 1987; 32, 231–244.
6. Ladizesky, N.H. and Pang, M.K.M. (1992) *Comp. Sci. Tech.*, 44, 127–136.
7. Xian, X.J. and Choy, C.L. Failure mechanisms in ultrahigh modulus polyethylene fiber reinforced composites, Proceedings of the Ninth International Conference on composite materials, Madrid, 1993; 12–16.
8. Porter, R.S. (1994) *Poly. Eng. Sci.*, 34, 266–8.
9. Sperling, L.H. Interpenetrating Polymeric Networks and Related Material. Plenum Press: New York, 1981.
10. Frisch, H.L., Frisch, K.C. and Klemmner, D. (1981) *Pure. App. Chem.*, 53, 1557–1566.
11. Zaks, Y., Lo, J., Raucher, D. and Pearce, E.M. (1982) *J. Appl. Polym. Sci.*, 27, 913–930.
12. Gardziella, A. (1990) *Kunst.*, 80(10), 1189–1192.
13. Freilich, M.A., Meiers, J.C., Duncan, J.P. and Goldberg, A.J. Fiber-reinforced Composites, Quintessence Publishing: Hong Kong, China, 9–21, 2000.
14. Hardy, R.L. (1971) *Geophys. Res.*, 176, 1905–1915.
15. Kansa, E.J. (1990) *Comput. Math. Appl.*, 19(8–9), 147–161.
16. Franke, R. (1982) *Math. Comput.*, 48, 181–200.
17. Coleman, C.J. (1996) *Comput. Mech.*, 17(6), 418–22.
18. Ferreira, A.J.M. (2003) *Mech. Adv. Mater. Struct.*, 10, 271–284.
19. Ferreira, A.J.M. (2003) *Comput. Struct.*, 59, 385–392.
20. Misra, R.K., Sandeep, K. and Misra, Ashok. (2007) *Int. J. Eng. Anal. Bound. Element.*, 31, 28–34.
21. Misra, R.K., Sandeep, K. and Misra, Ashok. (2007) *Int. J. Comput. Meth. Eng. Sci. Mech.*, 8, 1–10.
22. Franke, C. and Schaback, R. (1997) *Appl. Math. Comput.*, 93, 73–82.
23. Fedoseyev, A.I., Friedman, M.J. and Kansa, E.J. (2002) *Comput. Math Appl.*, 43(3–5), 491–500.
24. Misra, R.K., Sandeep, Kumar, Sandeep, K. and Misra, Ashok. (2008) *Composites.J. Mech. Mater. Struct.*, 3(1), 107–126.
25. Steiner, P.R. (1975) *J. Appl. Polym. Sci.*, 19(1), 215–225.
26. Rudin, A., Fyfe, C.A. and Vines, S.M. (1983) *J. Appl. Polym. Sci.*, 28(8), 2611–2622.
27. Melter, Y.L. Water Soluble Polymers Development Since 1978; Noyes Data Corporation; Park Ridge, NJ, 1981.
28. Peijs, A.A.J.M., Catsman, P., Govaert, L.E. and Lemstra, P.J. (1990) *Composites*, 21, 513.
29. Ladizesky, N.H. and Ward, I.M. (1983) *J. Mater. Sci.*, 18, 533.
30. Ladizesky, N.H. and Ward, I.M. (1989) *J. Mater. Sci.*, 24, 3763.
31. Silverstein, M.S. and Breuer, O. (1993) *J. Mater. Sci.*, 28, 4153.
32. Silverstein, M.S. and Breuer, O. (1993) *J. Mater. Sci.*, 28, 4718.
33. Andreopoulos, A.G., Liolios, K. and Patrikis, A. (1993) *J. Mater. Sci.*, 28, 5002.
34. Wolfrum, J. and Ehrenstein, G.W. (1995) *J. Appl. Polym. Sci.*, 74, 33173.
35. Datta, C., Basu, D. and Banerjee, A. (2002) *J. Appl. Poly. Sci.*, 86, 3581.
36. Ling, L. and Kansa, E.J. (2004) *Math. Comput. Modell.*, 40, 1413–1427.
37. Maity, J., Jacob, C., Das, C.K., Alam, S. and Singh, R.P. (2008) *Poly. Test.*, 27, 581–590.
38. Marais, C. and Feillard, B. (1992) *Compos. Sci. Tech.*, 45, 247–255.
39. Whitney, J.M. Structural analysis of laminated anisotropic plates, Technomic Publishing Company Inc: Lancaster, Pennsylvania, USA, 1987.
40. Chandrashekhara, K. Theory of plates, Universities Press (India) Limited: Hyderabad, India, 2001.

41. Pothan, L.A., Oommen, Z. and Thomas, S. (2003) *Composit. Sci. Tech.*, 63, 283–293.

**For clamped edge**

**Appendix**

**A. Multi-quadric radial basis function method for governing differential equation**

Substitution of multiquadric radial basis function in equation (5) gives:

$$\left( \sum_{j=1}^N w_j \frac{\partial^4}{\partial x^4} \varphi_j + 2R^2 \eta \sum_{j=1}^N w_j \frac{\partial^4}{\partial x^2 y^2} \varphi_j + \sum_{j=1}^n R^4 \psi w_j \frac{\partial^4}{\partial y^4} \varphi_j \right) + \sum_{j=1}^N w_j \frac{\partial^2}{\partial t^2} \varphi_j + C_v w_j \frac{\partial}{\partial t} \varphi_j - Q = 0 \tag{9}$$

Substitution of multi-quadric radial basis function in boundary conditions

**For Simple supported edge**

$$x = 0, a \sum_{j=1}^N w_j \varphi_j = 0 \tag{10a}$$

$$y = 0, b \sum_{j=1}^N w_j \varphi_j = 0 \tag{10b}$$

$$x = 0, a \sum_{j=1}^N w_j \frac{\partial^2}{\partial x^2} \varphi_j = 0 \tag{10c}$$

$$y = 0, b \sum_{j=1}^N w_j \frac{\partial^2}{\partial y^2} \varphi_j = 0 \tag{10d}$$

$$x = 0, a \sum_{j=1}^N w_j \varphi_j = 0 \tag{11a}$$

$$y = 0, b \sum_{j=1}^N w_j \varphi_j = 0 \tag{11b}$$

$$x = 0, a \sum_{j=1}^N w_j \frac{\partial}{\partial x} \varphi_j = 0 \tag{11c}$$

$$y = 0, b \sum_{j=1}^N w_j \frac{\partial}{\partial y} \varphi_j = 0 \tag{11d}$$

**B. Multiple regression analysis**

A.a = p

where

A = (l\*k) coefficient matrix

a = (k\*1) vector

p = (l\*1) load vector

Approximating the solution by introducing the error vector e, we get

$$p = Aa + e$$

where

e = (l\*1) vector

To minimize the error norm, let us define a function S as  $S(a) = e^T e = (p - Aa)^T (p - Aa)$

The least-square norm must satisfy

$$(\partial S / \partial a)_a = -2A^T p + 2A^T Aa = 0$$

This can be expressed as

$$a = (A^T A)^{-1} A^T P$$

or

$$a = B.P$$

The matrix B is evaluated once and stored for subsequent usages.